



Characterization of coarse bainite transformation in low carbon steel during simulated welding thermal cycles



Liangyun Lan^{a,b,*}, Xiangwei Kong^a, Chunlin Qiu^b

^a School of Mechanical Engineering and Automation, Northeastern University, Shenyang 110819, China

^b State Key Laboratory of Rolling Technology and Automation, Northeastern University, Shenyang 110819, China

ARTICLE INFO

Article history:

Received 12 January 2015

Received in revised form 2 May 2015

Accepted 4 May 2015

Available online 6 May 2015

Keywords:

Low carbon steel

Bainite transformation

Crystallography

Welding

Variant grouping

ABSTRACT

Coarse austenite to bainite transformation in low carbon steel under simulated welding thermal cycles was morphologically and crystallographically characterized by means of optical microscope, transmission electron microscope and electron backscattered diffraction technology. The results showed that the main microstructure changes from a mixture of lath martensite and bainitic ferrite to granular bainite with the increase in cooling time. The width of bainitic laths also increases gradually with the cooling time. For a welding thermal cycle with relatively short cooling time (e.g. $t_{8/5}$ is 30 s), the main mode of variant grouping at the scale of individual prior austenite grains changes from Bain grouping to close-packed plane grouping with the progress of phase transformation, which results in inhomogeneous distribution of high angle boundaries. As the cooling time is increased, the Bain grouping of variants becomes predominant mode, which enlarges the effective grain size of product phase.

© 2015 Elsevier Inc. All rights reserved.

1. Introduction

Understanding solid state phase transformation is of vital importance to design superior microstructures and to optimize mechanical properties of steel materials [1]. On the basis of the control of phase transformation, quite a number of novel steels have been developed to meet the increasing material demands for a variety of structural applications. For example, high grade pipeline steels are expected to have predominantly lower bainite with ultra-fine crystallographic domain via accelerated cooling process controlling phase transformation [2]. To maximize the amount of retained austenite in transformation-induced plasticity steels, a two-stage heat treatment with a bainitic isothermal transformation is usually employed and isothermal temperature is determined based on the T_0 curve for carbon enrichment [3].

It is well known that the crystallographic feature of microstructures, which is formed during the transformation, plays a vital role in low temperature toughness [4–7]. Large misorientation boundary can impede or even arrest the linear propagation of cleavage cracks, enhancing impact toughness of steels [6]. Thus, it is a hot issue how to obtain high density of large misorientation boundary (i.e., how to refine effective grain size which is defined as the size of region surrounded by the boundary with misorientation higher than 15 deg) during the phase transformation, especially for welding thermal cycle process. Guo et al. [8] determined that the effective grain size of the simulated heat affected zone (HAZ)

microstructure in low carbon steel reduces with a decrease in peak temperature and is smallest at the peak temperature of 900 °C, which is consistent with the change of impact toughness. In our previous study [9], the simulated coarse grained HAZ specimen with higher heat input has lower density of high angle boundary, which leads to the deterioration in impact toughness. In addition, the impact results for the specimens with middle heat input are discrete distribution. However, the nature of crystallographic evolution included in these phenomena above is still inconclusive.

In low carbon low alloy steels, the crystallography of phase transformation reveals that the orientation relationship between austenite (parent phase) and bainite or martensite (product phase) is close to the classic Kurdjumov–Sachs (K–S) relationship or others [10–14], although the actual orientation relationships between them are irrational [14]. In the K–S relationship maximum possible 24 different ferrite orientations (variants) can be formed within a single austenite grain. The variants having the same parallel close-packed planes relationship with austenite belong to the same type of crystallographic packet. Since there are only four sets of unique $\{111\}_\gamma$ planes, a maximum of four types of close-packed plane groups are present in the matrix [15]. Meanwhile, according to the lattice correspondence relations, these 24 variants can also be divided into three Bain groups in which all variants have a common $\{100\}_\alpha$ plane. The mode of variant grouping largely determines the misorientation of neighboring variants because the variants from the same Bain group are misoriented relative to each other by small angles.

Recently, many researches focused on the influencing factors of variant grouping, such as cooling rate, transformation temperature,

* Corresponding author at: P.O. Box 319, No. 11, Lane 3, Wenhua Road, HePing District, Shenyang 110819, China.

E-mail address: lanly@me.neu.edu.cn (L. Lan).

chemical composition and stress–strain field [13–20]. Takayama et al. [15] showed that the variants with Bain grouping are formed at higher isothermal temperatures, while the variants sharing the parallel close-packed plane occur at lower isothermal temperatures. Lambert-Perlade et al. [13] found that a crystallographic packet of bainite in low carbon steel during welding comprises variants belonging to a single Bain group. If the orientation of prior austenite grains is considered to be random after reheated by welding thermal cycle, the control of variant grouping mode should be an effective method to improve the density of high angle boundaries since the displacive transformation of products are confined to inside prior austenite grains. However, up to now, the variant grouping feature in low carbon steels during welding thermal cycle has only scarcely been studied at the scale of prior austenite grain level.

Consequently, in the present study, the simulated welding thermal cycle technique combined with interrupted cooling process by water quenching was employed to investigate the coarse austenite-to-bainite transformation in low carbon multi-microalloyed steel. The main focus is put on microstructure and crystallography of partial bainite transformation specimens to reveal the rule of crystallographic evolution (variant grouping within individual prior austenite grains) with the progress of welding thermal cycle.

2. Materials and experimental methods

The composition of steel plate chosen for this study was 0.053C, 0.25Si, 1.68Mn, 0.23Cr, 0.37Mo, 0.028Nb, 0.032V, 0.03Ti, and 0.0012B (wt.%). Welding thermal cycles were conducted on 6 mm diameter cylindrical samples using a thermo-mechanical simulator and a two dimensional Rykalin mathematical model was employed to simulate the thermal cycles of submerged arc welding. The experimental details are as follows: specimens were heated at a rate of 130 °C/s to a peak temperature of 1350 °C, and then immediately cooled with the $t_{8/5}$ cooling time from 5 to 600 s (the time for temperature to drop from 800 to 500 °C). The program was turned off manually after the phase change had finished, which produced complete continuous cooling transformation microstructures with a small amount of retained austenite at room temperature. The dilatation curves during heat treatment were recorded to obtain the transformation information. Fig. 1 shows the measured typical thermal cycle temperature curves.

To thoroughly reveal the evolution in the morphology and crystallography of bainite at the scale of prior austenite grains during the transformation, some of samples were water quenched immediately when the transformation reached to some specific volume fractions transformed (such as about 60% and 30% bainite formation when the

$t_{8/5}$ is 30 s with the quenching temperature of 450 °C and the $t_{8/5}$ is 120 s with the quenching temperature of 510 °C, respectively). They are referred to as partial bainite transformation microstructures. In Fig. 1, the solid red arrows represent schematically the water quenching processes.

The metallographic specimens were cut from the heat treatment region of interest and then polished by conventional techniques. Microstructural and crystallographic characteristics were examined using optical microscope, scanning electron microscope (ZEISS ULTRA 55) equipped with electron backscattered diffraction (EBSD) and transmission electron microscope (TEM, FEI Tecnai G² F20). The EBSD analysis focused on the samples with partial bainite transformation. The EBSD scanning area was about 280 × 250 μm with a step size of 0.5 μm to cover several prior austenite grains for lower heat input process. As regards higher heat input process (such as $t_{8/5}$ is 120 s), due to coarse prior austenite grain size the scanning area mainly focused on the transformed bainite region. Pattern-solving efficiencies for all EBSD maps were better than 80%. The 24 variants were sequentially numbered as per the method proposed by Morito et al. [10]. TEM foils, discs 3 mm in diameter, were cut from the continuous cooling transformation specimens and ground to a thickness of about 0.05 mm, and then twin-jet electropolished at a temperature of −30 °C with a voltage of 35 V.

3. Results and discussion

3.1. CCT diagram

Fig. 2 shows the microstructural morphology as a function of cooling time. As the cooling time is 5 s, the main microstructures are composed of lath martensite and bainitic ferrite. The carbides formed in bainitic ferrite are not very clear under optical microscope. As the cooling time increases to 85 s (Fig. 2b), the main microstructure is characterized by bainitic ferrite, accompanied with some granular bainite. Meanwhile, quite a number of carbides as well as martensite/austenite (MA) constituents are formed to decorate interlath boundaries of bainitic ferrite. Because bainite transformation always nucleates at the prior austenite grain boundaries and its growth is limited within the grains, the prior austenite grain boundaries are retained completely in the product phase, as signified with arrows in Fig. 2b. With further increase in cooling time, the main microstructure is fully changed into granular bainite. Fig. 2c shows the typical granular bainite which is characterized by coarse ferrite matrix and many massive MA constituents. These MA constituents distribute randomly in the matrix. In combination with the previous results [9], this kind of microstructure exhibits very low impact toughness due to the massive MA constituents and coarse ferrite matrix that favors the occurrence of complete cleavage fracture.

Fig. 3 represents the change of dilation with cooling temperature. The transformation-start temperature can be determined at the first point deviated from the linear portion of the dilatation curves, as signified with arrows. The transformation-finish temperatures are also confirmed with the same method. Comparing these two curves, the transformation temperature range rises with the increase in cooling time. Meanwhile, for the longer cooling time process ($t_{8/5}$ is 120 s), the transformation rate is very sluggish at the beginning stage, as circled in Fig. 3. This implies that the nucleation site of product phase is relatively rare and the growth rate is slow at higher transformation temperature [1]. This phenomenon is also related to variant grouping mode at the beginning of the transformation, which will be discussed later.

According to the information obtained from dilatometric curves and micrographs, the continuous cooling transformation (CCT) diagram can be established as shown in Fig. 4. The microstructure changes from granular bainite to a mixture of bainitic ferrite and granular bainite, further to a mixed lath martensite and bainitic ferrite with the decrease in cooling time. The polygonal ferrite cannot be formed even at the lowest cooling rate (e.g. $t_{8/5}$ is 600 s), which may be mainly attributed

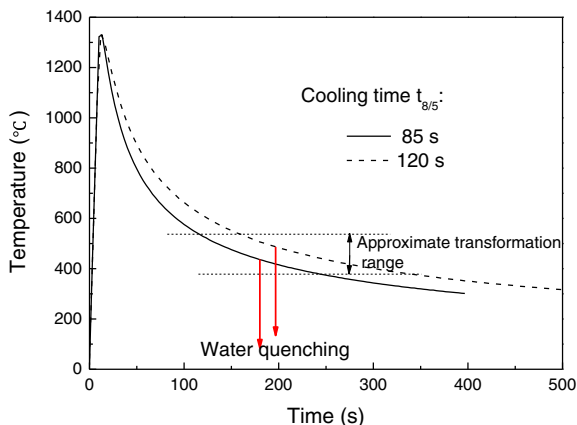


Fig. 1. Typical temperature curves of welding thermal cycles with different cooling times.

Download English Version:

<https://daneshyari.com/en/article/1570858>

Download Persian Version:

<https://daneshyari.com/article/1570858>

[Daneshyari.com](https://daneshyari.com)